



Published in final edited form as:

Cell Stem Cell. 2009 July 2; 5(1): 64–75. doi:10.1016/j.stem.2009.04.003.

***TAp63* prevents premature aging by promoting adult stem cell maintenance**

Xiaohua Su^{1,*}, Maryline Paris^{2,*}, Young Jin Gi¹, Kenneth Y. Tsai³, Min Soon Cho¹, Yu-Li Lin¹, Jeffrey A. Biernaskie², Satrajit Sinha⁴, Carol Prives⁵, Larysa H. Pevny⁶, Freda D. Miller², and Elsa R. Flores^{1,7}

¹Department of Molecular and Cellular Oncology, Graduate School of Biomedical Sciences, The University of Texas M.D. Anderson Cancer Center, 1515 Holcombe Blvd., Houston, TX 77030, USA

²Developmental and Stem Cell Biology Group, Hospital for Sick Children, Departments of Molecular Genetics and Physiology, University of Toronto, Toronto, Canada M5G1X5

³Departments of Dermatology and Immunology, The University of Texas M.D. Anderson Cancer Center, 1515 Holcombe Blvd., Houston, TX 77030, USA

⁴Department of Biochemistry, School of Medicine and Biomedical Sciences, State University of New York, Buffalo, NY 14214, USA

⁵Department of Biological Sciences, Columbia University, New York, NY 10027, USA

⁶Department of Genetics, University of North Carolina at Chapel Hill, NC 27599, USA

SUMMARY

The cellular mechanisms that regulate the maintenance of adult tissue stem cells are still largely unknown. We show here that the *p53* family member, *TAp63*, is essential for maintenance of epidermal and dermal precursors and that, in its absence, these precursors senesce and skin ages prematurely. Specifically, we have developed a *TAp63* conditional knockout mouse and used it to ablate *TAp63* in the germline (*TAp63*^{-/-}) or in K14-expressing cells in the basal layer of the epidermis (*TAp63*^{fl/fl};*K14cre*⁺). *TAp63*^{-/-} mice age prematurely and develop blisters, skin ulcerations, senescence of hair follicle-associated dermal and epidermal cells, and decreased hair morphogenesis. These phenotypes are likely due to loss of *TAp63* in dermal and epidermal precursors since both cell types show defective proliferation, early senescence, and genomic instability. These data indicate that *TAp63* serves to maintain adult skin stem cells by regulating cellular senescence and genomic stability, thereby preventing premature tissue aging.

INTRODUCTION

While the cellular mechanisms that regulate mammalian aging are still largely undefined, recent studies have suggested that aging can occur as a consequence of the functional depletion of somatic stem cells required for maintenance of adult tissues (Sharpless and

© 2010 II Press. All rights reserved.

⁷Correspondence to Elsa R. Flores. (elsaflores@mdanderson.org).

*Equal contribution.

Publisher's Disclaimer: This is a PDF file of an unedited manuscript that has been accepted for publication. As a service to our customers we are providing this early version of the manuscript. The manuscript will undergo copyediting, typesetting, and review of the resulting proof before it is published in its final citable form. Please note that during the production process errors may be discovered which could affect the content, and all legal disclaimers that apply to the journal pertain.

DePinho, 2007). Also, regenerative failure of tissues and premature aging arise in mice lacking genes critical for genomic stability and maintenance (Hasty et al., 2003). In this regard, the tumor suppressor *p53*, and its related family members, *p63* and *p73*, have all been linked to premature aging (Maier et al., 2004). Mice expressing a truncated mutant *p53* exhibit phenotypes associated with premature aging (Tyner et al., 2002), by a mechanism that is still under debate. Mice heterozygous for *p63* show premature aging (Flores et al., 2005; Keyes et al., 2005). However, in spite of the fact that *p53* regulates cellular senescence and genomic stability and the importance of these cellular functions to ensure adult stem cell longevity, the relationship between the two is still largely an open question.

p63 is critical for skin, limb, and nervous system development (Celli et al., 1999; Jacobs et al., 2005; Mills et al., 1999; Yang et al., 1999). Multiple roles have been identified for *p63* in the proliferation, differentiation, and maintenance of epidermal cells (Koster et al., 2007; Senoo et al., 2007). However, the analysis of *p63* function has been complicated by the presence of multiple isoforms of *p63* with various expression patterns in multiple tissues (Flores, 2007). The full-length TA isoforms contain a transactivation domain and structurally resemble *p53*, while the ΔN isoforms lack this domain and can act as dominant-negative family members. The existence of these isoforms has complicated the interpretation of the role of *p63* in multiple processes including its role as a tumor suppressor (Flores, 2007; Flores et al., 2005). With regard to the epidermis, the functions of the TA and ΔN isoforms of *p63* have been examined by overexpression or knock down in early differentiating keratinocytes (Candi et al., 2006; Koster et al., 2007). These studies, together with the high relative expression of $\Delta Np63$ in the epidermis suggest that the $\Delta Np63$ and not *TAp63* isoforms are critical for epidermal development and maintenance. More recently, a *TAp63*^{-/-} mouse was created showing that this isoform is critical for protection of the female germline (Suh et al., 2006). However, these approaches have not demonstrated a specific role for *TAp63* in the epidermis, nor have they addressed a potential role for *p63* in the mesenchymal compartment of the skin or other epithelial tissues that are affected in the *p63*^{-/-} mice.

To understand the role of *TAp63* in skin development, we generated a conditional knock out allele of *TAp63* in the mouse, and used transgenic mice expressing the cre recombinase in the germline (Zp3-cre and protamine-cre) (Lewandoski et al., 1997; O'Gorman et al., 1997) or in the epidermis (K14cre) (Jonkers et al., 2001) to target genetic ablation of *TAp63*. We found that mice generated with germline deletion of *TAp63* (*TAp63*^{-/-}) develop blisters, ulcerated wounds, decreased wound healing, and accelerated aging. Surprisingly, our data indicate that these phenotypes were due to the loss of *TAp63* in a dermal precursor population that resides within a hair follicle niche (Fernandes et al., 2004; Toma et al., 2001; J. Biernaskie, L. Pevny, and F.D. Miller, unpublished observations). The loss of *TAp63* in these dermal precursors (termed SKPs for skin-derived precursors) led to hyperproliferation, senescence, and genomic instability in culture, and premature senescence and reduced hair follicle morphogenesis in vivo. In addition to these dermal deficits, cultured *TAp63*^{-/-} epidermal cells displayed decreased colony formation, increased senescence, and genomic instability. Together, these findings indicate that *TAp63* serves to maintain adult tissue stem cells thereby preventing premature aging, and to provide direct evidence that *TAp63* has an important role in regulating cellular senescence and genomic stability.

EXPERIMENTAL PROCEDURES

Generation of *TAp63* conditional knockout mice

The cre-loxP strategy was used to generate the *TAp63* conditional knockout allele (*TAp63^{fl}*). Genomic *p63* DNA from intron 1 to 3 was amplified from BAC clone DNA (BAC RP23-186N8, Children's Hospital Oakland Research Institute). LoxP sites flanking

exon 2 and neomycin (*neo*) gene flanked by *frt* sites inserted in intron 2 were cloned into pL253 (Liu et al., 2003). ES cells were analyzed by Southern blot analysis. Chimeras resulting from ES cell clones injected into C57BL/6 blastocysts were mated with C57BL/6 albino females, and genotyped as described below. Mice with germline transmission of the targeted allele (conditional, floxed allele) were crossed with Zp3-Cre (C57BL/6) (Lewandoski et al., 1997) or Protamine-Cre (C57BL/6 × 129S6) (O'Gorman et al., 1997) transgenic mice. All procedures were approved by the IACUC at U.T. M.D. Anderson Cancer Center and by the Hospital for Sick Children Care Committee and were within the guidelines of the Canadian Council of Animal Care.

Blister Analysis

Thirty wild-type and *Tap63*^{-/-} mice housed individually were observed throughout life for macroscopic phenotypic changes. Mice were sacrificed at 1, 2, and 4 months for blister characterization. Immunocytochemistry was performed using anti-collagen IV (1:80, Abcam) and anti-K14 (1:2000, Dennis Roop) followed by Texas Red-conjugated goat anti-rabbit and FITC conjugated goat anti-guinea pig secondary antibodies (1:1000, Jackson ImmunoResearch).

Wound healing assay

Mice were anesthetized and two 5 mm diameter full thickness punch wounds were made on each side of the dorsum using Acu-Punch (Acuderm Inc.). Mice were housed individually and wounds were measured at days 0, 1, 2, 4, and 6. At day 6, mice were euthanized and one half of the epithelium was fixed in 10% formalin and the other frozen in OCT medium (Tissue Tek). 1.2 mg/kg buprenorphine was injected subcutaneously for pain management.

Primary keratinocyte isolation and colony formation

Cells were isolated from skin of P1 mice or embryos at day 18.5 (E18.5) by treatment with DispaseII (Roche). The separated epidermis was minced and incubated in 0.25% trypsin/EDTA (GIBCO) for 20 minutes. Cells were plated on collagen-coated flasks (50 µg/ml) collagen type I (BD Bioscience) in defined K-SFM medium (GIBCO). 5×10^3 cells were plated on 60mm dishes containing mitomycin c (Roche)-treated J2 3T3 feeder cells in F media as described (Barrandon and Green, 1987). Colonies cultured for 8, 12, or 20 days were fixed in 10% formalin, and stained with 2% rhodamine B (Sigma) or with the following antibodies: anti-cytokeratin 5 (Abcam) (1:1000), anti-cytokeratin 10 (Chemicon) (1:1000), and anti-gamma-H2AX-FITC (Upstate Biotechnology)(1:100). Secondary antibodies used were FITC- or Texas Red-conjugated (Jackson ImmunoResearch)(1:500). Some dishes were treated with 10 mM BrdU for 15 hours and immunostained for BrdU (Becton Dickinson). Apoptotic cells were detected with the FragEL kit (Calbiochem).

SKP Isolation and culture

Dorsal and whisker pad skin were removed from E18 embryos, young (1 month), or aged (12 months) mice as described previously (Biernaskie et al., 2006). To transfect SKPs, 25,000 cells were plated on coated (1% Poly-D Lysine and 1% Laminin) chamber slides and transfected with pCMV-p57^{Kip2} or pCMV-EGFP expression vectors using the Fugene reagent. 48hrs after transfection, cells were fixed in 4% paraformaldehyde and analyzed for expression of p57^{Kip2} and Ki67 by immunocytochemistry

Sox2-EGFP sorted cells

Dorsal skin samples from adult (n=3) Sox2-EGFP mice (Ellis et al., 2004) were enzymatically digested. Viable cells were gated. Sox2-EGFP-negative, Sox2-EGFP-positive,

or total live cells were collected by flow cytometry using a MoFlo (Dako) cell sorter and analyzed by RT-PCR.

Cytogenetics

Primary keratinocytes treated with colcemid (0.02 mg/ml) and fixed in 75% methanol / 25% acetic acid were dropped onto slides and stained with 5.0% Giemsa in PBS (pH 6.8). Images were processed with MetaMorph Premier (Molecular Devices) using a Nikon Eclipse E400 microscope.

Statistics

All data are represented as mean \pm SEM. Data were analyzed using one-way ANOVA test or student's *t*-test for comparison between two groups. A p-value of 0.05 was considered significant. All experiments were done at least in triplicate.

RESULTS

Generation of a TAp63 conditional knockout mouse

We generated a *TAp63* conditional knock out mouse (*TAp63^{fl}*) using the cre-loxP system (Fig. 1) allowing for tissue specific deletion of the *TAp63* isoforms and retention of the $\Delta Np63$ isoforms. LoxP sites were inserted in to the *p63* gene flanking exon 2, which contains the translational start site of the *TAp63* isoforms, to generate a floxed allele (*TAp63^{fl}*) (Fig. 1A). Properly targeted embryonic stem (ES) cells were injected into donor blastocysts and subsequently into pseudopregnant females. Resulting male chimeras were intercrossed with albino C57/B6 females for germline transmission scored by PCR and Southern blot analysis (Fig. 1B & C).

Generation of a TAp63^{-/-} mouse

To further understand the role of *TAp63* in skin development, a *TAp63^{-/-}* mouse was generated by intercrossing the *TAp63^{fl}* mouse (*TAp63^{fl/fl}*) with germline-specific cre transgenic mice (Zp3-cre and protamine-cre)(Lewandoski et al., 1997; O'Gorman et al., 1997). We detected embryonic lethality (35%) on an enriched C57B/6 background (~95%) but not upon subsequent backcrossing to the 129S6 strain. Quantitative RT-PCR performed on keratinocytes isolated from *TAp63^{-/-}* newborn mice confirmed absence of *TAp63* mRNA ($p < 0.0001$) (Fig. 1D) or protein expression (Fig. 1F) with maintenance of wild-type levels of $\Delta Np63$ mRNA (Fig. 1E) and protein (Fig. 1G) throughout embryonic development.

TAp63^{-/-} mice develop blisters, ulcerated wounds, and accelerated signs of aging

The *TAp63^{-/-}* mice that survived to birth exhibited small skin blisters in early adulthood and signs of accelerated aging at later stages, including ulcerated wounds, and premature death (Fig. 1H). By one month of age, 33% of *TAp63^{-/-}* mice developed blisters that ultimately led to ulcerated wounds on their dorsal and ventral sides (Figs. 1H-K). Keratin 14 and collagen IV immunostaining revealed a subepidermal split between the basement membrane and the dermis with accumulation of entrapped serum (Figs. 1I & K). While the blisters themselves are not likely a sign of premature aging, the wounds that result from these ruptured blisters progress to severe skin ulcerations that fail to heal with aging (Fig. 1H). The other 66% of the cohort developed blisters and ulcerations by 2 to 4 months. In addition, the *TAp63^{-/-}* mice exhibited signs of premature aging. By X-ray analysis, we found that twenty-five percent of *TAp63^{-/-}* mice (n=28) developed kyphosis by 8 months and 86% developed this condition by 10 months compared to 14% in the wild-type mice at 10 months (n=29) (Fig. 1L). Defects in other epithelial tissues were also noted within the

kidney, stomach, esophagus, and bladder leading to the development of multiple cysts in these tissues. Finally, the median lifespan of the *TAp63*^{-/-} mice was only 333 days compared to 712 days for wild-type mice (n=28) (p<0.001) (Fig. 1M).

One possible explanation for these premature aging phenotypes is that *TAp63* is essential for maintenance of the adult precursor populations that maintain tissues. To address this possibility, we determined whether p63 was expressed in the dermis in addition to its reported expression in epidermal precursors and keratinocytes (Senoo et al., 2007). Immunocytochemical analysis of adult skin for p63 and antibodies specific for epidermal versus dermal cells demonstrated that p63 was expressed in epidermal cells of the hair follicle, where it was localized to the nucleus (Fig. 2A). However, it was also expressed in the fibronectin-positive dermal sheath (DS) cells of the hair follicle and in a subpopulation of NCAM-positive dermal papilla cells, where it was localized to the cytoplasm (Fig. 2A), as has been reported in other cell types (Kurita et al., 2005). To confirm this result, we took advantage of the finding that hair follicle DP and DS cells express a Sox2:EGFP reporter, and are the only cells to do so within adult backskin from the mouse (J. Biernaskie, L. Pevny, and F.D. Miller, unpublished observations). Following isolation of Sox2:EGFP-positive cells by cell sorting from Sox2:EGFP mice (Ellis et al., 2004), RT-PCR analysis demonstrated that *TAp63* was expressed in these cells (Fig. 2B), and therefore, in follicle DP and DS cells. *TAp63* was also expressed in the negative fraction, presumably in the Sox2-negative epidermal cells. Since the follicle dermal sheath and the related dermal papilla are niches for skin-derived precursors (SKPs), an adult dermal precursor population implicated in hair follicle morphogenesis and dermal maintenance (Fernandes et al., 2004; J. Biernaskie, L. Pevny, and F.D. Miller, unpublished observations), then this suggests that p63 is expressed in precursor cell populations in both the dermis and epidermis.

To determine whether *TAp63* is essential for maintenance of these precursor populations, we stained sections of young adult skin (1 month) for senescence-associated β -galactosidase (SA- β -gal), a marker for cellular senescence. SA- β -gal staining was undetectable in sections of young wild-type skin (Fig. 2C), but was localized to the bulge region, the dermal sheath, and papilla of hair follicles in *TAp63*^{-/-} mice (Suppl. Fig. 1 & Fig. 2C). Quantification demonstrated a 15-fold increase in total SA- β -gal-positive hair follicles (Suppl. Fig. 1B) and a 2-fold increase in hair follicles with SA- β -gal-positive dermal papillae in young *TAp63*^{-/-} skin (Fig. 2D). Interestingly, similar SA- β -gal staining in follicle dermal cells was observed in aged wild-type skin at 12 months (Fig. 2D), suggesting that in the absence of *TAp63*, precursor cells senesce prematurely.

To investigate whether this premature senescence has functional consequences, we quantified hair follicles in backskin from *TAp63*^{-/-} and wild-type mice at 1 to 12 months. Young mice of both genotypes and wild-type skin at all ages had a similar density of hair follicles (7–8 hair follicles/mm) that were uniformly distributed over the entirety of the backskin (Fig. 2E & F). In contrast, aged (6–12 month) *TAp63*^{-/-} skin exhibited many areas where there were no hair follicles at all (Fig. 2E) interspersed with areas where the hair follicle density was similar to that of wild-type mice (Fig. 2E). We measured the percentage of skin lacking hair follicles across gaps of greater than 400 μ m. This analysis demonstrated that, at 1 month, hair was evenly distributed along the backskin of both wild-type and *TAp63*^{-/-} mice, with virtually no gaps (Fig. 2E–G). By 6–12 months, occasional hairless patches were noted in the wild-type mice, occurring as part of the normal aging process. In contrast, 30–40% of the *TAp63*^{-/-} backskin was hairless by 6–12 months (Fig. 3G).

To determine whether this age-dependent hair follicle loss was due to immune-mediated destruction of hair follicles, skin from 27 *TAp63*^{-/-} mice and 12 wild-type mice aged 1 to 12 months were examined. No perifollicular lymphocytic infiltrates composed of T-cells

were apparent in these samples. Additionally, in autoimmune diseases where hair follicles are destroyed, affected areas show perifollicular scarring (fibrosis) as well as fibrous tracts that mark areas where intact follicles once stood (Ackerman, 1997). None of the samples examined showed such evidence. To further confirm that this hair follicle loss was not due to immune-mediated destruction, we immunostained sections for the T-cell marker (CD3) and for the macrophage marker (Iba-1). Immunostaining for the T cell marker, CD3, was performed on 11 *TAp63*^{-/-} and 3 WT mice at early time points (less than 6 months of age) (Suppl. Fig. 2) and demonstrated no significant differences in lymphocytic infiltrates or evidence of active follicular injury. Similar results were obtained with immunostaining for the macrophage marker Iba-1 (Suppl. Fig. 3), indicating that the blistering and hair follicle loss seen in *TAp63*^{-/-} mice was not due to an aberrant immune attack. These data, together with the skin ulceration phenotype observed in *TAp63*^{-/-} mice, indicate that *TAp63* is essential for maintenance of both epidermal and dermal stem cell populations, and that in its absence, there are patches of skin where hair follicles are absent and large skin ulcers form, due to premature aging/senescence of these precursors.

TAp63 is essential for wound healing

Adult tissue stem cells are essential not only for tissue maintenance, but also for appropriate wound-healing responses. To assess whether this skin ulceration phenotype was due to aberrant wound-healing, we performed a wound-healing assay using wild-type and *TAp63*^{-/-} mice at one month (Fig. 3A & B). Five millimeter punch wounds were made on the dorsal side of wild-type and *TAp63*^{-/-} mice, and six days later, wound sizes were measured. Wounds in *TAp63*^{-/-} mice had not healed and were almost twice as large as those in wild-type mice (Fig. 3A–C). Consistent with these findings, BrdU incorporation in the epidermis of *TAp63*^{-/-} mice was less than half of that in wild-type mice (Fig. 3D–F). Similarly, levels of BrdU incorporation were low in the dermis of wounded *TAp63*^{-/-} mice (Fig. 3K). Thus, *TAp63* is necessary to ensure appropriate dermal and epidermal wound-healing responses.

Deletion of TAp63 in K14-positive cells is not sufficient to recapitulate the TAp63^{-/-} phenotypes

To determine whether these skin phenotypes were due to the loss of *TAp63* in the epidermal compartment, we first asked whether TAp63 was expressed in epidermal cells in vivo. Consistent with previous studies (Koster et al., 2004), TAp63 was not detected in the intact epidermis of wild-type mice. However, when skin was wounded and double-labeled for TAp63 and keratin 5, a marker for the basal layer of the epidermis, scattered epidermal cells within the wound site of wild-type mice expressed TAp63 (Fig. 3G–J) indicating its induction in response to stress. Indeed, wild-type passage 2 keratinocytes exhibited an induction of TAp63 while freshly isolated keratinocytes (passage 0) did not (Fig. 3M). To determine whether epidermal *TAp63* is essential for appropriate wound-healing, we generated mice with a selective deletion of *TAp63* in the epidermal compartment using keratin 14 (K14) cre transgenic mouse (Jonkers et al., 2001), which expresses the cre-recombinase in the basal layer of the epidermis. Consequently, dermal, but not epidermal, cells in these mice are wild-type. Quantitative RT-PCR analysis of epidermal cells derived from the intact epidermis of *TAp63^{fl/fl};K14cre* mice at E18.5 showed that TAp63 mRNA was not detectable, similar to what was seen with epidermal cells derived from *TAp63*^{-/-} mice (Fig. 3L). To confirm that TAp63 was deleted in epidermal cells from *TAp63^{fl/fl};K14cre* mice, we derived keratinocytes from *TAp63^{fl/fl};K14cre*, passaged them in culture, and then performed Western blots (Fig. 3N). This analysis demonstrated that TAp63 was induced and detectable in cultured wild-type keratinocytes, as was p53 (Fig. 3M), but that no TAp63 was observed in passaged keratinocytes cultured from *TAp63^{fl/fl};K14cre* mice (Fig. 3N). These results indicate that most epidermal cells from *TAp63^{fl/fl};K14cre* mice extracted at E18.5 do not express TAp63, although it is possible that cre-mediated excision of the

floxed allele is incomplete in epidermal cells, particularly given the low endogenous levels of TAp63 expression.

Interestingly, *TAp63^{fl/fl};K14^{cre}* mice did not display any overt skin phenotypes under normal conditions suggesting that loss of *TAp63* in K14-expressing epidermal cells alone was insufficient to cause the skin ulcerations seen in *TAp63^{-/-}* mice. To further address this issue, we performed punch biopsies on the *TAp63^{fl/fl};K14^{cre}* mice. Analysis of wound-healing revealed that *TAp63^{fl/fl};K14^{cre}* and wild-type mice healed their wounds at similar rates (Fig. 3C). Likewise, the levels of BrdU incorporation in the epidermis and dermis of *TAp63^{fl/fl};K14^{cre}* mice were similar to those in wild-type mice (Fig. 3F & K). Together, these data suggest that loss of *TAp63* in most keratinocytes is not sufficient to recapitulate the skin ulceration or wound-healing deficit observed in *TAp63^{-/-}* mice.

TAp63 is essential for colony formation from epidermal precursors

Since *p63* has been implicated in the proliferation of epidermal stem cells (Senoo et al., 2007), we asked whether this phenotype was due to loss of *TAp63*. We isolated and cultured epidermal cells from newborn wild-type and *TAp63^{-/-}* mice (Fig. 4A) (Barrandon and Green, 1987), analyzed colonies at 8, 12, and 20 days to observe their proliferative and self renewal capacities. Wild-type cells generated colonies containing keratin 5 (K5) positive immature keratinocytes, the majority of which contained up to 50% BrdU-positive proliferating cells at 8 and 20 days (Fig. 4A–D). In contrast, *TAp63^{-/-}* epidermal cells generated small, irregular-shaped colonies of K5-positive cells, the majority of which contained no proliferating cells at 8 or 20 days (Fig. 4A–D). In spite of this perturbation in colony formation, cells within these *TAp63^{-/-}* colonies differentiated and expressed keratin 10, a marker of the spinous layer of the epidermis, following treatment with high calcium (Fig. 4E). This deficit in colony formation is similar to that seen with knockdown of all *p63* isoforms in epidermal precursors (Senoo et al., 2007), and indicates that *TAp63* is required for epidermal precursor proliferation and/or the appropriate genesis of proliferation-competent keratinocytes.

We also performed similar experiments with epidermal cells isolated from *TAp63^{fl/fl};K14^{cre}* mice (Fig. 4A–D). These cells formed colonies and proliferated like wild-type epidermal cells. These data are consistent with the lack of skin phenotypes in the *TAp63^{fl/fl};K14^{cre}* mice.

Since the *p53* family members interact extensively, we asked whether this colony formation phenotype could be rescued by coincident loss of *p53*. Thus, colony formation assays were performed with epidermal cells isolated from *TAp63^{-/-};p53^{-/-}* mice (Fig. 4A). Eight days after culture, *p53* deletion partially rescued the *TAp63^{-/-}* phenotype; wild-type and *TAp63^{-/-};p53^{-/-}* epidermal cells generated similar numbers of colonies with 50% or fewer proliferating cells, but only 18% of *TAp63^{-/-};p53^{-/-}* colonies ($p=0.038$) had >50% BrdU positive cells compared to 28% of wild-type and 6% of *TAp63^{-/-}* colonies ($p=0.020$) (Fig. 4C). This rescue was not, however, apparent at 20 days, when *TAp63^{-/-};p53^{-/-}* colonies were similar to *TAp63^{-/-}* colonies, and statistically different from wild-type colonies (Fig. 4D). Thus, coincident loss of *p53* partially rescued the *TAp63^{-/-}* colony formation phenotype at short but not long culture time points (Fig. 4A, C, & D).

TAp63 regulates self-renewal of dermal precursor cells

These data suggest that the skin phenotypes in *TAp63^{-/-}* mice require the loss of *TAp63* in dermal cells. We therefore asked whether *TAp63* regulated SKPs, dermal precursors within a niche in the hair follicle where *p63* is expressed (Fig. 2A & B). We isolated wild-type SKPs and characterized the repertoire of *p53* family members expressed by RT-PCR.

Consistent with the expression of p63 in hair follicle Sox2:EGFP-positive dermal cells in vivo (Fig. 2A & B), SKPs expressed detectable *TAp63* mRNA (Fig. 5A), but not $\Delta Np63$ or *p73*. *p53* levels were similar in SKPs that were isolated from the dermis of *p63*^{-/-} and wild-type embryos (Fig. 5A & B). Immunostaining for p63 confirmed that SKPs isolated from neonatal dermis or hair follicles expressed detectable p63 protein (Fig. 5C). Thus, of the *p53* family members, SKPs express only *TAp63* and *p53*, and expression of *p53* family members is not dysregulated by the absence of *p63*.

To determine whether *TAp63* is necessary for maintenance of SKPs, we isolated them from 1 month *TAp63*^{-/-} and wild-type skin. Immunocytochemical analysis of SKP spheres for fibronectin, nestin, vimentin, and versican, all markers that have been defined for SKPs (Biernaskie et al., 2006; Fernandes et al., 2004; Toma et al., 2001) demonstrated that there were no overt differences in expression of these SKP markers with the loss of *TAp63* (Fig. 5D). However, immunostaining for the proliferation marker Ki67 demonstrated that *TAp63*^{-/-} SKPs isolated from young mice proliferated approximately 4–5-fold more than wild-type counterparts (Fig. 5F). Similar results were obtained when SKPs were isolated from the rudimentary dermis of E18 *p63*^{-/-} embryos (Fig. 5E, F). To determine if this increased proliferation reflected increased self-renewal, SKPs were dissociated to single cells, plated at low density in medium containing methylcellulose, and the percentage of cells that initiated a new sphere was determined. As seen in the proliferation assay, SKPs cultured from postnatal *TAp63*^{-/-} and E18 *p63*^{-/-} mice self-renewed 3–4 times more robustly than did wild-type SKPs (Fig. 5G). In spite of this hyperproliferation, *TAp63*^{-/-} and wild-type SKPs were still able to differentiate into both neural and mesodermal cell types under previously defined conditions (Suppl. Fig. 4A) and when transplanted into the neural crest migratory stream of embryonic chicks in ovo at HH stage 18, both populations of SKPs migrated into neural crest targets (Suppl. Fig. 4B) (Fernandes et al., 2004). Thus, *TAp63* regulates SKP proliferation and self-renewal, but does not overtly affect their phenotype, differentiation, or migratory capacity.

These data suggest that *TAp63* normally functions to dampen the self-renewal rate of SKPs, potentially as a mechanism for ensuring that they last for the lifetime of the animal. One p63 target that decreases cellular proliferation is the cyclin-dependent kinase inhibitor p57^{Kip2} (Beretta et al., 2005). RT-PCR analysis demonstrated that *p57^{Kip2}* mRNA levels were reduced in *TAp63*^{-/-} and *p63*^{-/-} SKPs (Fig. 5H). Immunocytochemistry confirmed this result, and demonstrated that while p57^{Kip2} was robustly expressed in 50% of wild-type SKPs, it was only detectably expressed in 18% of *TAp63*^{-/-} SKPs (Fig. 5I,J). In contrast, RT-PCR for two other cell cycle regulators, *p27^{Kip1}* and *p21^{Cip1}* demonstrated unchanged expression in the absence of *p63* (Suppl. Fig. 4C). Chromatin immunoprecipitation for p63 identified a previously-defined binding site in the *p57^{Kip2}* promoter (Fig. 5K). We therefore asked if the hyperproliferation phenotype in *TAp63*^{-/-} SKPs could be rescued by p57^{Kip2}. Following transfection of *TAp63*^{-/-} SKPs with either empty vector or *p57^{Kip2}*, 20% of cells transfected with *p57^{Kip2}* expressed detectable levels of this protein, and none of these transfected cells coexpressed Ki67 (Fig. 5L). In contrast, approximately 45% of *TAp63*^{-/-} cells transfected with the empty vector were dividing, as monitored by Ki67, and none of them expressed p57^{Kip2} (Fig. 5L). Thus, *p57^{Kip2}* completely rescued the hyperproliferation, indicating that *TAp63* regulates SKPs self-renewal at least in part by regulating *p57^{Kip2}*.

Loss of TAp63 causes dermal precursors to senesce

To investigate whether *TAp63*^{-/-} precursors senesce, SKPs were generated from 1 month *TAp63*^{-/-} and wild-type skin and analyzed for expression of SA- β -gal and p16^{Ink4a}, a second marker for senescence that is associated with human aging (Sharpless and DePinho, 2007). SA- β -gal staining demonstrated that a very large proportion of the cells in *TAp63*^{-/-} SKP spheres were SA- β -gal-positive (Fig. 6A). Similarly, immunostaining for p16^{Ink4a}

revealed that over 50% of the cells in SKP spheres were p16^{Ink4a}-positive versus less than 10% of the wild-type SKPs (Fig. 6B & C). Interestingly, analysis of SKPs generated from aged wild-type skin demonstrated that 50–60% of the SKPs were also p16^{Ink4a}-positive (Fig. 6B), supporting the notion that SKPs normally senesce as animals age, and that loss of *TAp63* causes premature aging.

Since *TAp63*^{-/-} SKPs show both hyperproliferation and increased senescence, we immunostained spheres for both Ki67 and p16^{Ink4a}. This analysis demonstrated that these two proteins were expressed in different populations of cells (Fig. 6B), consistent with the idea that as SKPs senesce, they exit the cell cycle. Interestingly, however, approximately 5% of *TAp63*^{-/-} SKPs expressed both Ki67 and p16^{Ink4a}, and in these cells, their subcellular distribution within the nucleus was mutually exclusive (Fig. 6D), indicating that these cells represent a transition state between hyperproliferation and senescence. These data are consistent with the interpretation that *TAp63* serves to maintain SKPs in a largely quiescent state, and that in its absence, SKPs hyperproliferate and ultimately senesce, thereby causing premature dermal and follicle aging.

To ask whether *TAp63* is a more general regulator of cellular senescence, we examined cultured epidermal cells for SA-β-gal. *TAp63*^{-/-} cells had a dramatic increase in SA-β-gal relative to wild-type cells (Fig. 6E). To determine whether this cellular senescence required *p53*, we intercrossed the *p53*^{-/-} (Jacks et al., 1994) and *TAp63*^{-/-} mice. Analysis of *TAp63*^{-/-};*p53*^{-/-} cells revealed that, somewhat surprisingly, the number of SA-β-gal-positive cells was further increased by the coincident loss of *p53* (Fig. 6E). In contrast, apoptosis, which was increased in the absence of *TAp63*, was rescued by coincident deletion of *p53*; 0% of cultured *TAp63*^{-/-};*p53*^{-/-} cells underwent apoptosis compared to 18% of *TAp63*^{-/-} and 6% of wild-type cells (Fig. 6F). Consequently, the increase of senescence in the *TAp63*^{-/-};*p53*^{-/-} cells may be due to the coincident decrease in apoptosis. Taken together, these data suggest that *TAp63* may be a general regulator of cellular senescence, and indicate that the senescence in these cells is *p53*-independent.

Loss of *TAp63* results in DNA damage and genomic instability

One known trigger for cellular senescence is DNA damage. In light of the wound-healing deficits and cellular senescence seen in *TAp63*^{-/-} mice, we asked whether *TAp63*^{-/-} skin cells might have accumulated DNA damage. Immunostaining for histone γH2AX, which is induced during DNA damage, on SKPs and epidermal cells from wild-type and *TAp63*^{-/-} mice revealed that 70–80% of 1 month-old *TAp63*^{-/-} SKPs expressed this DNA damage marker (Fig. 7A & B), whereas none of the age-matched controls did. Likewise, *TAp63*^{-/-} epidermal cells had a marked increase in γH2AX nuclear foci. One hundred percent of *TAp63*^{-/-} cells were γH2AX positive compared to less than 5% of wild-type cells (Fig. 7D). To confirm the presence of genomic instability *in vivo*, we immunostained young and aged skin for γH2AX. Young wild-type skin showed virtually no γH2AX-positive cells, but aged skin showed a small population of positive cells in the dermal sheath of hair follicles (Fig. 7C). In contrast, in 1 month-old *TAp63*^{-/-} skin, γH2AX-positive cells were consistently observed in the dermal sheath (Fig. 7C).

Because of the strikingly high levels of DNA damage, we assayed for chromosomal instability. More than 100 metaphase spreads from primary wild-type and *TAp63*^{-/-} epidermal cells were scored for chromosomal aberrations. *TAp63*^{-/-} cells had a large number of cytogenetic aberrations including chromosomal fusions, fragments, breaks, banded chromosomes, ring chromosomes, dicentric chromosomes, and aneuploidy (Fig. 7E), suggesting that *TAp63* is a critical for maintenance of genomic stability.

DISCUSSION

Here, we show that *TAp63* plays an instrumental role in the maintenance and renewal of dermal and epidermal precursors, and when this function is perturbed, it causes premature aging of both the precursors themselves and the tissues that they maintain. We demonstrated this by generating a conditional knockout allele of *TAp63*, preserving the $\Delta Np63$ isoforms, and intercrossing it with germline or epidermal specific cre transgenic mice. Mice with a germline deletion of *TAp63* developed blisters, ulcerated wounds, display decreased wound healing, and an accelerated aging phenotype. Surprisingly, these phenotypes were at least partially due to the loss of *TAp63* in SKPs, dermal precursors that reside within a hair follicle niche. Loss of *TAp63* in SKPs led to hyperproliferation, senescence, and genomic instability in culture, and premature senescence and reduced hair follicle morphogenesis *in vivo*. In addition to these dermal deficits, cultured *TAp63*^{-/-} epidermal precursors displayed decreased colony formation, as previously seen with *p63*^{-/-} epidermal precursors (Senoo et al., 2007), a phenotype that is likely at least partially due to increased senescence and genomic instability, as we show here. Together, these findings indicate that *TAp63* serves to regulate and maintain the adult stem cells that are essential to prevent premature skin aging, and provide direct evidence that *TAp63* has a physiologically important role in regulating cellular senescence and genomic stability.

TAp63^{-/-} mice exhibited signs of premature aging including hair loss, impaired wound healing, kyphosis, and a median lifespan of only 48 weeks compared to 110 weeks for their wild-type littermates. Intriguingly, premature aging has also been seen in mice mutant for *p53* (Tyner et al., 2002) and in *p63*^{+/-} mice (Flores et al., 2005; Keyes et al., 2005). Strikingly, the life span of *TAp63* knockout mice is approximately half of that seen with *p63*^{+/-} mice (Flores et al., 2005; Keyes et al., 2005) suggesting that the *p63*^{+/-} aging phenotype is largely attributable to loss of *TAp63*. It is also tempting to speculate that *p53* mouse models that display premature aging may do so via *TAp63*. Two mouse models expressing truncated p53 mutants display premature aging (Maier et al., 2004; Tyner et al., 2002), but other mouse models with elevated p53, the super p53 and *mdm2^{puro}/Δ7-12* mice (Garcia-Cao et al., 2002; Mendrysa et al., 2006), do not. Perhaps these truncated p53 mutants bind to and inhibit TAp63, thereby causing premature aging. Precedent for such an interaction comes from mouse models of Li-Fraumeni Syndrome (Iwakuma et al., 2005; Lang et al., 2004) and from *in vitro* studies with point mutant p53 (Iwakuma et al., 2005).

How does *TAp63* regulate aging? Our data indicate that it does so by regulating the maintenance of adult tissue stem cells. In particular, we demonstrate that in the absence of *TAp63* *in vivo*, hair follicle dermal precursors display premature senescence, show signs of DNA damage, and lose their ability to induce hair follicle morphogenesis. Moreover, since follicle-associated precursors also contribute to dermal maintenance and wound-healing (J. Biernaskie, L. Pevny, and F.D. Miller, unpublished observations), then deficits in this same population may account for the wound healing and skin ulceration phenotypes seen in *TAp63*^{-/-} mice. In addition, epidermal precursors are highly deficient in colony formation likely contributing to the skin phenotypes we document here. Moreover, we show that *TAp63* is essential to keep epidermal cells from senescing and to maintain their genomic integrity. Thus, two adult skin precursor populations depend upon *TAp63* for their maintenance, and we propose that the loss of *TAp63* leads to functional depletion of both populations, resulting in premature skin aging. These findings provide significant support for the concept that depletion of adult stem cells may be a major cause of tissue aging (Sharpless and DePinho, 2007), and raise the possibility that functional depletion of adult stem cells is responsible for the phenotypes of humans with dysregulated TAp63 (Gu et al., 2006).

At the cellular level, our data provide a number of TAp63-dependent mechanisms that explain depletion of adult stem cell function. First, *TAp63*^{-/-} SKPs showed increased proliferation and self-renewal in culture, a phenotype that correlated with decreased expression of p57^{Kip2}, a direct transcriptional target of p63 (Beretta et al., 2005). Since adult stem cell populations are not immortal, enhanced proliferation of follicle-associated SKPs would be predicted to lead to stem cell depletion. Interestingly, re-expression of p57^{Kip2} in *TAp63*^{-/-} SKPs rescued the hyperproliferative phenotype of *TAp63*^{-/-} SKPs indicating that regulation of p57^{Kip2} by TAp63 is essential in the maintenance of these dermal precursors. Second, in the absence of *TAp63*, both SKPs and epidermal cells displayed greatly increased DNA damage and chromosomal aberrations indicating a key role for *TAp63* in regulating genomic stability and stem cell maintenance. Third, in the absence of *TAp63*, both SKPs and epidermal cells displayed greatly increased senescence, something that was also seen *in vivo*. *TAp63* might directly regulate cellular senescence, as does p53, or this senescence might occur in response to DNA damage or telomere shortening as a consequence of hyperproliferation. The senescence induced by TAp63 is largely p53-independent suggesting a unique senescence pathway regulated by TAp63. Regardless of the trigger, senescence would withdraw stem cells from the cell cycle, thereby effectively depleting them. All three mechanisms may be at play in the stem cell maintenance/premature aging phenotypes that are observed in *TAp63*^{-/-} mice.

The phenotype of the *TAp63*^{fl/fl};*K14cre* mice was strikingly different from that of the *TAp63*^{-/-} mice. The *TAp63*^{fl/fl};*K14cre* mice healed their wounds at similar rates to wild-type mice and had similar numbers of BrdU positive cells in the dermal and epidermal compartments. Additionally, epidermal cells derived from *TAp63*^{fl/fl};*K14cre* mice proliferated similarly to wild-type epidermal cells. There are a number of possible explanations for these data. First, the loss of *TAp63* in epidermal cells may not be sufficient for the deficits that are reported here; deletion of *TAp63* in both dermal and epidermal precursors might be required. Second, our results might be due to incomplete deletion of *TAp63* in the *TAp63*^{fl/fl};*K14cre* mice. However, our data demonstrating that *TAp63* mRNA is not detectable in primary embryonic epidermal cells by quantitative RT-PCR argues that recombination has occurred in most epidermal cells by E18.5. Finally, these deficits may require the loss of *TAp63* in an embryonic epidermal precursor prior to the onset of *K14cre* expression. Our data do not distinguish between these possibilities.

The *p63* deficient mouse has craniofacial abnormalities and lacks stratified epithelium resulting in death within hours after birth. Since this *p63*^{-/-} mouse model lacks all isoforms of *p63*, it has been difficult to specifically attribute these deficits to any particular mechanism. One exception to this has been in the embryonic peripheral nervous system, where neurons only express TAp63 isoforms, and where these isoforms act as essential proapoptotic proteins during naturally-occurring cell death (Jacobs et al., 2005). The role of the TAp63 isoforms has been less clear in the skin. The ΔN isoforms, most notably $\Delta Np63\alpha$, are highly expressed in the basal layer of the epithelium, leading to the assumption that they are responsible for the effects of p63 on proliferation of epidermal precursors and development of the epidermis. Support for this idea comes from genetic complementation experiments where *TAp63* α and $\Delta Np63\alpha$ were expressed in K5-positive cells in transgenic mice; expression of $\Delta Np63\alpha$ showed a more impressive rescue of the epidermis than did *TAp63* α (Candi et al., 2006). Our data are consistent with this conclusion, since *TAp63*^{-/-} mice do not display the same developmental skin phenotype as *p63*^{-/-} mice. Our data using mouse models indicate that *TAp63* is important for skin maintenance, primarily by acting in dermal and epidermal precursors. Importantly, the *TAp63*^{-/-} mice display a phenotype similar to defects in humans with Hay-Wells syndrome where patients with mutations in *p63* develop dermatitis and alopecia (McGrath et al.,

2001). Thus, *TAp63* and $\Delta Np63$ might each play important roles in the skin via actions in different compartments at different developmental time points.

In addition to its critical role in stem cell maintenance, TAp63 is induced in response to stress. This is reminiscent of the induction of TAp63 in sympathetic neurons following growth factor withdrawal (Jacobs et al., 2005) and of p53 after DNA damage. Since we also observe a DNA damage response and chromosomal instability in *TAp63*^{-/-} cells, then one possibility is that TAp63 is induced with p53 as an essential part of a stress response to protect the genome. Further support for this idea comes from previous reports that *TAp63* plays a key role in maintaining the fidelity of the female germline (Suh et al., 2006), and that *p63* can act as a tumor suppressor gene (Flores, 2007; Flores et al., 2005). Thus, *TAp63* likely acts with *p53* and to maintain genomic integrity, thereby protecting long-lived cells like stem cells, and potentially suppressing tumorigenesis. Interestingly, mouse models with accumulated DNA damage, such as the ATR^{mKO} mouse exhibit age-related phenotypes (Ruzankina et al., 2007), supporting the idea that genomic instability in tissue stem cells is one way that the loss of *TAp63* causes premature aging.

In summary, the findings reported here indicate that *TAp63* serves to maintain the adult stem cells that are required for skin maintenance, thereby preventing premature aging. *TAp63* does this by regulating precursor cell proliferation, maintaining genomic integrity, and preventing premature cellular senescence. Whether *TAp63* or the related *TAp73* play similar roles in other adult stem cell populations, and whether *TAp63* regulates genomic integrity or cellular senescence in other normal or tumorigenic cells are key questions for the future.

Supplementary Material

Refer to Web version on PubMed Central for supplementary material.

Acknowledgments

This work was supported by grants to E.R.F. from the American Cancer Society (RSG-07-082-01-MGO), March of Dimes (Basil O'Connor Scholar), Susan G. Komen Foundation (BCTR600208), Leukemia and Lymphoma Society / Hildegard D. Becher Foundation, NCI-Cancer Center Core Grant (CA-16672)(U.T. M.D. Anderson Cancer Center) and by grants to F.D.M. from the Canadian Institutes of Health Research (MOP-64211) and HHMI. E.R.F. is a scholar of the Rita Allen Foundation and the V Foundation for Cancer Research. F.D.M. is a Canada Research Chair and an HHMI International Research Scholar. We gratefully acknowledge the work of Jan Parker-Thornburg, the Genetically Engineered Mouse Facility, and the T.C. Hsu Molecular Cytogenetics Core at M.D. Anderson (funded by NCI #CA16672). We would also like to acknowledge Wei Zhang for technical assistance, Paul Lambert and Denis Lee for J2-3T3 feeder cells, Dennis Roop for K14 antibody, Alea Mills for *p63*^{-/-} mice, Elaine Fuchs for advice on wound-healing assays, David Kaplan and Chi-chung Hui for advice and input with regard to the manuscript.

REFERENCES

- Ackerman, AB. Histologic Diagnosis of Inflammatory Skin Diseases. 2nd Ed.. Baltimore, MD: Williams & Wilkins; 1997.
- Barrandon Y, Green H. Three clonal types of keratinocyte with different capacities for multiplication. Proceedings of the National Academy of Sciences of the United States of America. 1987; 84:2302–2306. [PubMed: 2436229]
- Beretta C, Chiarelli A, Testoni B, Mantovani R, Guerrini L. Regulation of the cyclin-dependent kinase inhibitor p57Kip2 expression by p63. Cell Cycle. 2005; 4:1625–1631. [PubMed: 16258268]
- Biernaskie JA, McKenzie IA, Toma JG, Miller FD. Isolation of skin-derived precursors (SKPs) and differentiation and enrichment of their Schwann cell progeny. Nat Protoc. 2006; 1:2803–2812. [PubMed: 17406538]

- Candi E, Rufini A, Terrinoni A, Dinsdale D, Ranalli M, Paradisi A, De Laurenzi V, Spagnoli LG, Catani MV, Ramadan S, et al. Differential roles of p63 isoforms in epidermal development: selective genetic complementation in p63 null mice. *Cell Death and Differentiation*. 2006; 13:1037–1047. [PubMed: 16601749]
- Celli J, Duijf P, Hamel BC, Bamshad M, Kramer B, Smits AP, Newbury-Ecob R, Hennekam RC, Van Buggenhout G, van Haeringen A, et al. Heterozygous germline mutations in the p53 homolog p63 are the cause of EEC syndrome. *Cell*. 1999; 99:143–153. [PubMed: 10535733]
- Ellis P, Fagan BM, Magness ST, Hutton S, Taranova O, Hayashi S, McMahon A, Rao M, Pevny L. SOX2, a persistent marker for multipotential neural stem cells derived from embryonic stem cells, the embryo or the adult. *Dev Neurosci*. 2004; 26:148–165. [PubMed: 15711057]
- Fernandes KJ, McKenzie IA, Mill P, Smith KM, Akhavan M, Barnabe-Heider F, Biernaskie J, Junek A, Kobayashi NR, Toma JG, et al. A dermal niche for multipotent adult skin-derived precursor cells. *Nat Cell Biol*. 2004; 6:1082–1093. [PubMed: 15517002]
- Flores ER. The roles of p63 in cancer. *Cell Cycle*. 2007; 6:300–304. [PubMed: 17264676]
- Flores ER, Sengupta S, Miller JB, Newman JJ, Bronson R, Crowley D, Yang A, McKeon F, Jacks T. Tumor predisposition in mice mutant for p63 and p73: Evidence for broader tumor suppressor functions for the p53 family. *Cancer Cell*. 2005; 7:363–373. [PubMed: 15837625]
- Flores ER, Tsai KY, Crowley D, Sengupta S, Yang A, McKeon F, Jacks T. p63 and p73 are required for p53-dependent apoptosis in response to DNA damage. *Nature*. 2002; 416:560–564. [PubMed: 11932750]
- Garcia-Cao I, Garcia-Cao M, Martin-Caballero J, Criado LM, Klatt P, Flores JM, Weill JC, Blasco MA, Serrano M. "Super p53" mice exhibit enhanced DNA damage response, are tumor resistant and age normally. *EMBO J*. 2002; 21:6225–6235. [PubMed: 12426394]
- Gu X, Lundqvist EN, Coates PJ, Thurffjell N, Wettersand E, Nylander K. Dysregulation of TAp63 mRNA and protein levels in psoriasis. *J Invest Dermatol*. 2006; 126:137–141. [PubMed: 16417229]
- Hasty P, Campisi J, Hoeijmakers J, van Steeg H, Vijg J. Aging and genome maintenance: lessons from the mouse? *Science*. 2003; 299:1355–1359. [PubMed: 12610296]
- Iwakuma T, Lozano G, Flores ER. Li-Fraumeni syndrome: a p53 family affair. *Cell Cycle*. 2005; 4:865–867. [PubMed: 15917654]
- Jacks T, Remington L, Williams BO, Schmitt EM, Halachmi S, Bronson RT, Weinberg RA. Tumor spectrum analysis in p53-mutant mice. *Curr Biol*. 1994; 4:1–7. [PubMed: 7922305]
- Jacobs WB, Govoni G, Ho D, Atwal JK, Barnabe-Heider F, Keyes WM, Mills AA, Miller FD, Kaplan DR. p63 is an essential proapoptotic protein during neural development. *Neuron*. 2005; 48:743–756. [PubMed: 16337913]
- Jonkers J, Meuwissen R, van der Gulden H, Peterse H, van der Valk M, Berns A. Synergistic tumor suppressor activity of BRCA2 and p53 in a conditional mouse model for breast cancer. *Nat Genet*. 2001; 29:418–425. [PubMed: 11694875]
- Keyes WM, Wu Y, Vogel H, Guo X, Lowe SW, Mills AA. p63 deficiency activates a program of cellular senescence and leads to accelerated aging. *Genes & Development*. 2005; 19:1986–1999. [PubMed: 16107615]
- Koster MI, Dai D, Marinari B, Sano Y, Costanzo A, Karin M, Roop DR. p63 induces key target genes required for epidermal morphogenesis. *Proceedings of the National Academy of Sciences of the United States of America*. 2007; 104:3255–3260. [PubMed: 17360634]
- Koster MI, Kim S, Mills AA, DeMayo FJ, Roop DR. p63 is the molecular switch for initiation of an epithelial stratification program. *Genes & Development*. 2004; 18:126–131. [PubMed: 14729569]
- Kurita T, Cunha GR, Robboy SJ, Mills AA, Medina RT. Differential expression of p63 isoforms in female reproductive organs. *Mech Dev*. 2005; 122:1043–1055. [PubMed: 15922574]
- Lang GA, Iwakuma T, Suh YA, Liu G, Rao VA, Parant JM, Valentin-Vega YA, Terzian T, Caldwell LC, Strong LC, et al. Gain of function of a p53 hot spot mutation in a mouse model of Li-Fraumeni syndrome. *Cell*. 2004; 119:861–872. [PubMed: 15607981]
- Lewandoski M, Wassarman KM, Martin GR. Zp3-cre, a transgenic mouse line for the activation or inactivation of loxP-flanked target genes specifically in the female germ line. *Curr Biol*. 1997; 7:148–151. [PubMed: 9016703]

- Liu P, Jenkins NA, Copeland NG. A highly efficient recombineering-based method for generating conditional knockout mutations. *Genome Res.* 2003; 13:476–484. [PubMed: 12618378]
- Maier B, Gluba W, Bernier B, Turner T, Mohammad K, Guise T, Sutherland A, Thorner M, Scrable H. Modulation of mammalian life span by the short isoform of p53. *Genes & Development.* 2004; 18:306–319. [PubMed: 14871929]
- McGrath JA, Duijf PHG, Doetsch V, Irvine AD, de Waal R, Vanmolkot KRJ, Wessagowit V, Kelly A, Atherton DJ, Griffiths WAD, et al. Hay–Wells syndrome is caused by heterozygous missense mutations in the SAM domain of p63. *Hum Mol Genet.* 2001; 10:221–229. [PubMed: 11159940]
- Mendrysa SM, O'Leary KA, McElwee MK, Michalowski J, Eisenman RN, Powell DA, Perry ME. Tumor suppression and normal aging in mice with constitutively high p53 activity. *Genes & Development.* 2006; 20:16–21. [PubMed: 16391230]
- Mills AA, Zheng B, Wang XJ, Vogel H, Roop DR, Bradley A. p63 is a p53 homologue required for limb and epidermal morphogenesis. *Nature.* 1999; 398:708–713. [PubMed: 10227293]
- O'Gorman S, Dagenais NA, Qian M, Marchuk Y. Protamine-Cre recombinase transgenes efficiently recombine target sequences in the male germ line of mice, but not in embryonic stem cells. *Proceedings of the National Academy of Sciences of the United States of America.* 1997; 94:14602–14607. [PubMed: 9405659]
- Ruzankina Y, Pinzon-Guzman C, Asare A, Ong T, Pontano L, Cotsarelis G, Zediak VP, Velez M, Bhandoola A, Brown EJ. Deletion of the developmentally essential gene ATR in adult mice leads to age-related phenotypes and stem cell loss. *Cell Stem Cell.* 2007; 1:113–126. [PubMed: 18371340]
- Senoo M, Pinto F, Crum CP, McKeon F. p63 Is essential for the proliferative potential of stem cells in stratified epithelia. *Cell.* 2007; 129:523–536. [PubMed: 17482546]
- Sharpless NE, DePinho RA. How stem cells age and why this makes us grow old. *Nat Rev Mol Cell Biol.* 2007; 8:703–713. [PubMed: 17717515]
- Suh EK, Yang A, Kettenbach A, Bamberger C, Michaelis AH, Zhu Z, Elvin JA, Bronson RT, Crum CP, McKeon F. p63 protects the female germ line during meiotic arrest. *Nature.* 2006; 444:624–628. [PubMed: 17122775]
- Toma JG, Akhavan M, Fernandes KJ, Barnabe-Heider F, Sadikot A, Kaplan DR, Miller FD. Isolation of multipotent adult stem cells from the dermis of mammalian skin. *Nat Cell Biol.* 2001; 3:778–784. [PubMed: 11533656]
- Tyner SD, Venkatachalam S, Choi J, Jones S, Ghebranious N, Igelmann H, Lu X, Soron G, Cooper B, Brayton C, et al. p53 mutant mice that display early ageing-associated phenotypes. *Nature.* 2002; 415:45–53. [PubMed: 11780111]
- Yang A, Schweitzer R, Sun D, Kaghad M, Walker N, Bronson RT, Tabin C, Sharpe A, Caput D, Crum C, et al. p63 is essential for regenerative proliferation in limb, craniofacial and epithelial development. *Nature.* 1999; 398:714–718. [PubMed: 10227294]

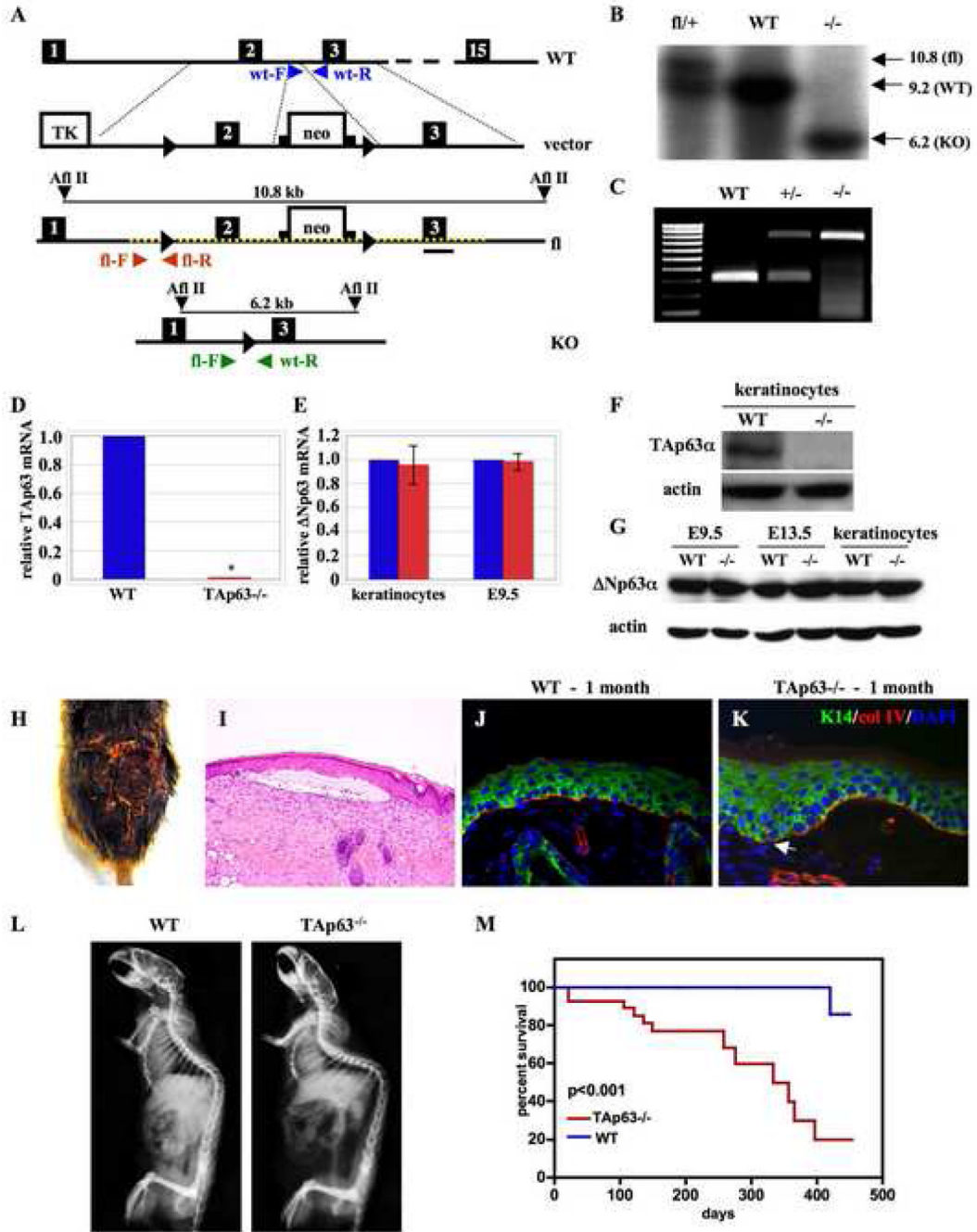


Figure 1. TAp63^{-/-} mice develop blisters and exhibit accelerated aging phenotypes
 (A) Generation of the *TAp63* conditional knockout mice. The *TAp63* targeting vector was generated by inserting loxP sites (triangles) flanking exon 2 and a neomycin (neo) cassette flanked by *f*rt sites (squares) in intron 2. Primers used for genotyping by PCR of wild-type (blue) and *TAp63* conditional knockout (fl) (red) alleles are shown. The targeted region of the floxed allele is depicted by a dashed yellow line. (B) Southern blot analysis of genomic DNA from *TAp63^{fl/+}*, WT, and *TAp63^{-/-}* mice. (C) PCR of DNA from wild-type (WT), *TAp63^{+/-}* (+/-) and *TAp63^{-/-}* (-/-) mice. (D, E) Quantitative RT-PCR of (D) *TAp63* mRNA from wild-type (WT) and *TAp63^{-/-}* keratinocytes or of (E) $\Delta Np63$ mRNA from wild-type (blue) and *TAp63^{-/-}* (red) keratinocytes and day 9.5 (E9.5) embryos. GAPDH

was used as an internal control. (F, G) Western blot for TAp63 (F) in wild-type (WT) and *TAp63*^{-/-} passage 2 keratinocytes or for Δ Np63 (G) in wild-type (WT) and *TAp63*^{-/-} E9.5 and E13.5 embryos and keratinocytes. Actin was used as an internal control. (H) Dorsum of an 8-month *TAp63*^{-/-} mouse with an ulcerated wound. (I) H&E cross section of skin from a 1 month *TAp63*^{-/-} mouse with a blister. Arrows indicate the split at the epidermal-dermal junction with entrapped serum. (J, K) Immunocytochemistry for keratin 14 (green) and collagen IV (red) of skin from 1 month wild-type (J) and *TAp63*^{-/-} mice (K). DAPI was used as a counterstain. Magnification 200X. White arrow indicates the beginning of the dermal/epidermal separation. N=6 mice per group. (L) X-ray of 8 month wild-type (WT) and *TAp63*^{-/-} mice. (M) Kaplan-Meier survival curve for wild-type (WT) and *TAp63*^{-/-} mice. Median survival for *TAp63*^{-/-} and WT mice is 333 and 712 days, respectively, n=29 mice per group, p<0.001.

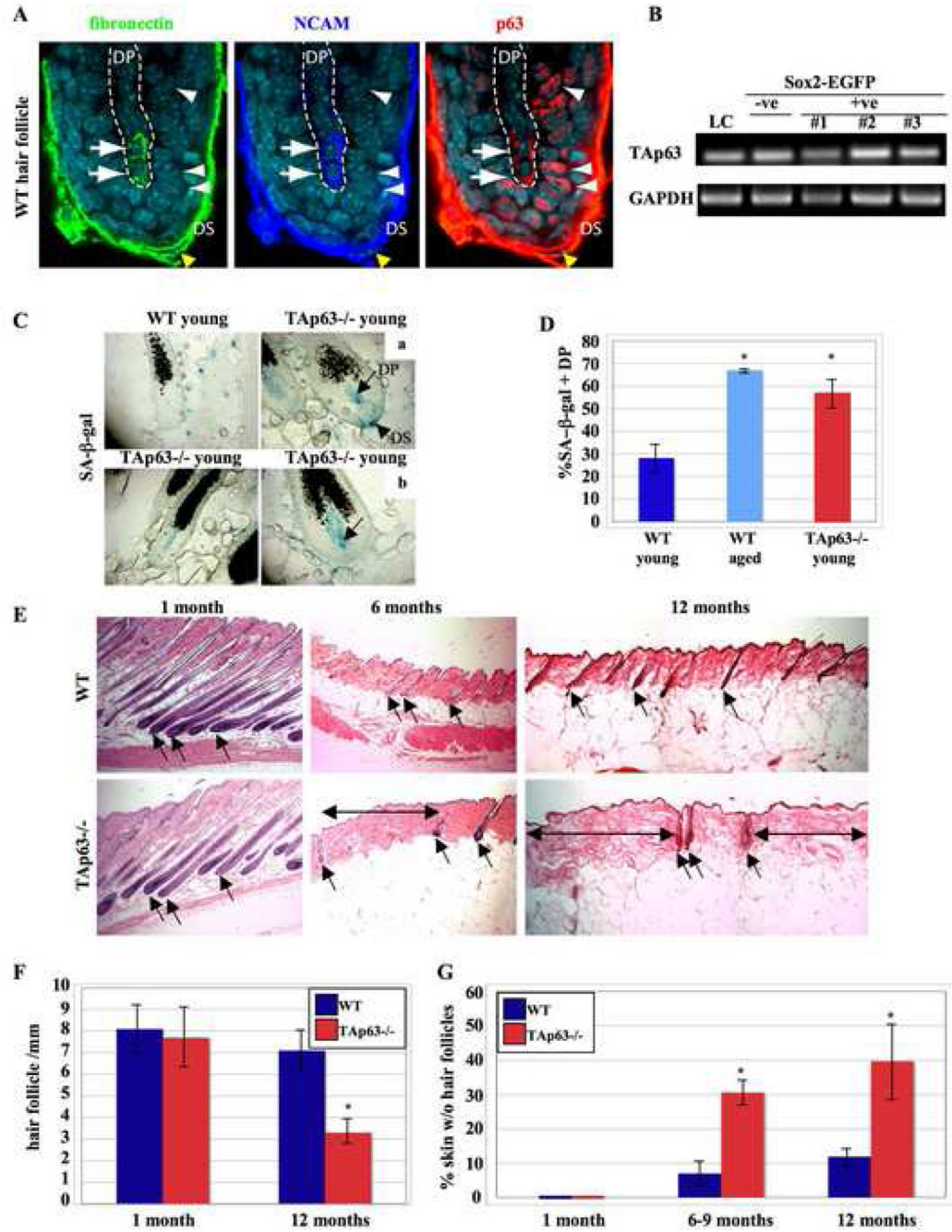


Figure 2. TAp63^{-/-} mice lose hair follicles with age

(A) Confocal images of immunocytochemistry of a hair follicle from a young, wild-type mouse for fibronectin (green), NCAM (dark blue), p63 (red), and Hoechst 33258 (blue). Hatched line denotes the dermal papilla (DP), yellow arrowhead indicates a p63-positive dermal sheath (DS) cell, arrows show a p63-positive dermal papilla cells, and white arrowheads epidermal cells with nuclear p63. Magnification 630X. (B) RT-PCR for *TAp63* mRNA in Sox2:EGFP-positive (+ve) and negative (-ve) cells from adult backskin. #1, 2 and 3 are samples from 3 different mice, and the ungated sample is total skin cells from one mouse. (C) SA-β-gal staining (blue) of hair follicles in young wild-type or *TAp63*^{-/-} skin (left two panels). The arrows indicate SA-β-gal-positive dermal papillae. The right two

panels, (a) and (b), are micrographs of sequential sections through the same hair follicle, 40 μ m apart. The arrowhead indicates an SA- β -gal-positive dermal sheath cell (DS), and the arrows a positive dermal papilla (DP). (D) Quantification of SA- β -gal positive cells in the dermal papillae (DP). n = 3 animals per group. *p<0.05. (E) H&E stained skin sections of 1, 6, and 12 month wild-type (WT) and *TAp63*^{-/-} mice. Arrows denote hair follicles, and double-arrows indicate regions of *TAp63*^{-/-} skin depleted of hair follicles. Magnification 100X. (F) Quantification of hair follicles per millimeter (E). N = 8 and 4 mice each for wild-type (WT) and *TAp63*^{-/-} at 1 month and 12 months, respectively. *p<0.05. (G) Quantification of hair follicles in wild-type (WT) and *TAp63*^{-/-} mice at 1, 6–9, and 12 months. Only patches of skin with no follicles for greater than 400 μ m were included. N = 4 mice of each genotype at each time point. *p<0.05.

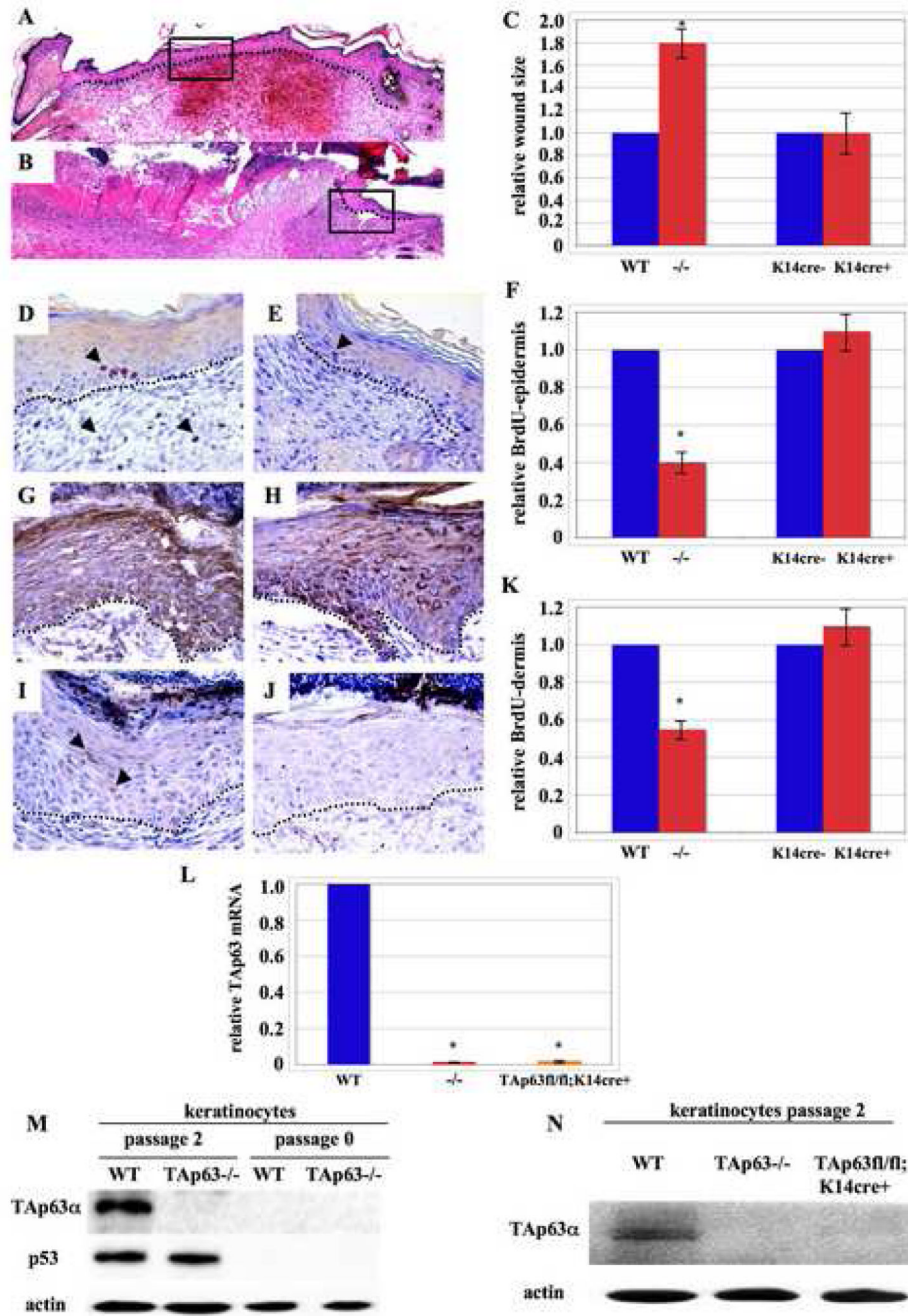


Figure 3. *TAp63*^{-/-} mice have an impaired wound-healing response

(A,B) Photomicrographs of wild-type (A) and *TAp63*^{-/-} (B) H&E stained skin sections 6 days after wounding. Dotted lines indicate the dermal-epidermal boundary and boxes denote area of immunohistochemical analysis on serial sections shown at higher magnification in panels D, E, G, H, I, & J. (C) Bar graph indicating relative wound size 6 days after wounding in wild-type (WT), *TAp63*^{-/-} (*-/-*), *TAp63*^{fl/fl}; *K14cre*⁻ (*K14cre*⁻), and *TAp63*^{fl/fl}; *K14cre*⁺ (*K14cre*⁺) mice. N=6 mice per group, *p<0.05. (D,E) Immunohistochemistry for BrdU incorporation 6 days after wounding in wild-type (D) and *TAp63*^{-/-} (E) mice. (F) Quantification of BrdU incorporation in epidermal cells in sections shown in panels D,E in WT, *TAp63*^{-/-}, *TAp63*^{fl/fl}; *K14cre*⁻, and *TAp63*^{fl/fl}; *K14Cre*⁺

mice. N=6 mice per group, *p<0.001. (G–J) Immunohistochemistry for keratin 5 (G,H; brown) or TAp63 (I,J; brown) in wild-type (G,I) or *TAp63*^{-/-} (H,J) skin. (K) Quantification of BrdU incorporation in dermal cells. In panels (D, E, G, H, I, J), tissue was counterstained with hematoxylin. Arrowheads denote BrdU positive dermal and epidermal cells (D, E) and TAp63-positive epidermal cells (I). N=6 mice per genotype. (L) qRT-PCR of mRNA from WT, *TAp63*^{-/-}, and *TAp63*^{fl/fl};*K14cre*⁺ epidermal cells extracted from E18.5 skin. N=6 mice per genotype in triplicate. (M) Western blots for TAp63 and p53 in stressed keratinocytes (passage 2) and freshly-isolated keratinocytes (passage 0) from wild-type (WT) and *TAp63*^{-/-} mice. (N) Western blot for TAp63 in WT, *TAp63*^{-/-}, and *TAp63*^{fl/fl};*K14cre*⁺ stressed keratinocytes (passage 2). Actin was used as an internal control. Keratinocytes derived from 3 independent embryos for each genotype and performed in triplicate.

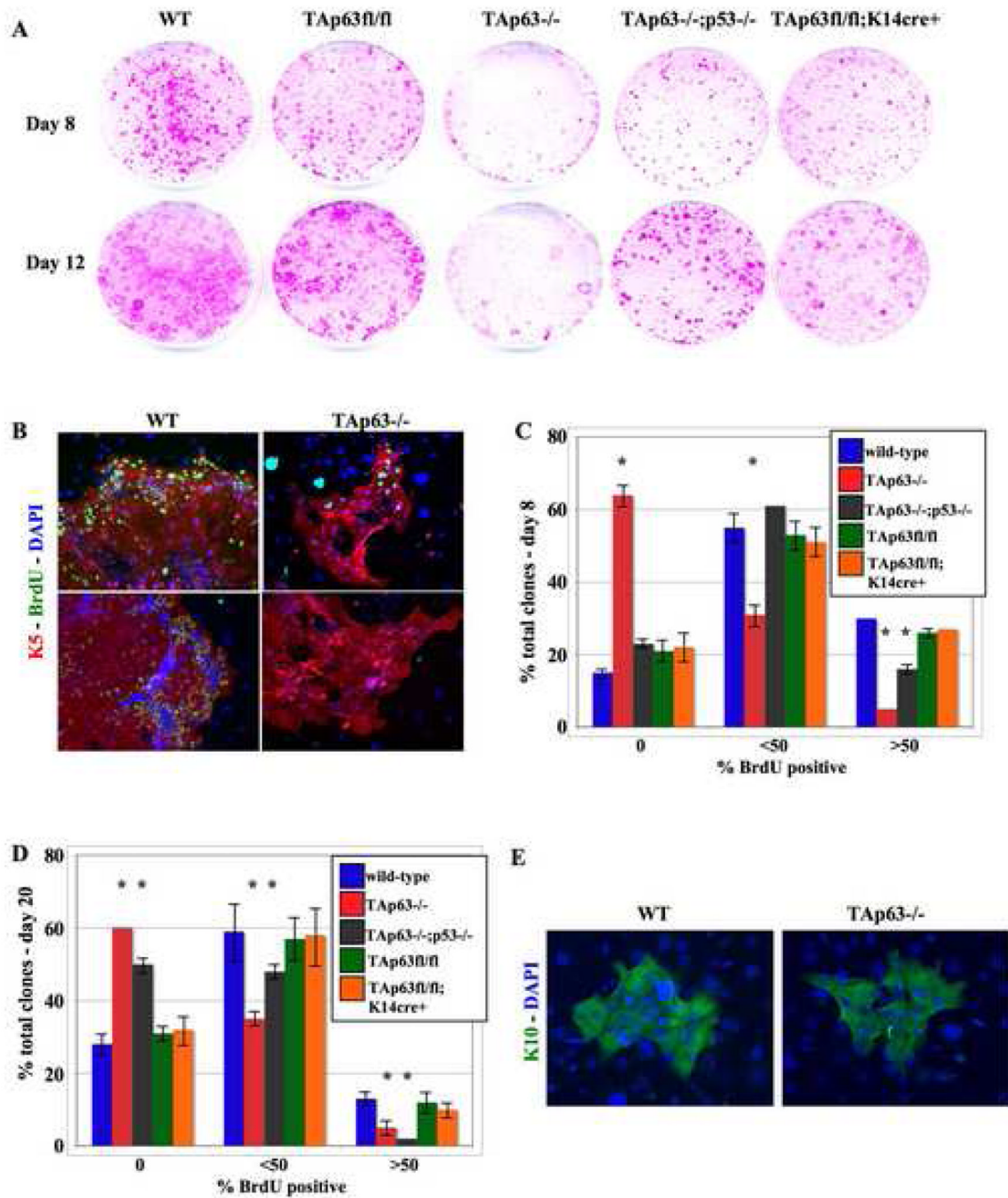


Figure 4. TAp63 regulates colony formation from epidermal precursors

(A) Epidermal colonies from wild-type (WT), *TAp63fl/fl*, *TAp63-/-*, *TAp63-/-;p53-/-* and *TAp63fl/fl;K14Cre+* mice cultured for 8 or 12 days on J2 3T3 feeder layers and stained with rhodamine B. (B) Immunostaining for BrdU (green) and K5 (red) in wild-type and *TAp63-/-* epidermal clones. (C,D) Quantification of BrdU incorporation in colonies after 8 (C) or 20 (D) days in culture. * $p < 0.05$. $N = 3$ cell lines per genotype in triplicate. (E) Immunostaining for the spinous marker, K10 (green), in wild-type (WT) and *TAp63-/-* colonies cultured in high calcium (1.2 mM) media for 2 days. DAPI was used as a counterstain.

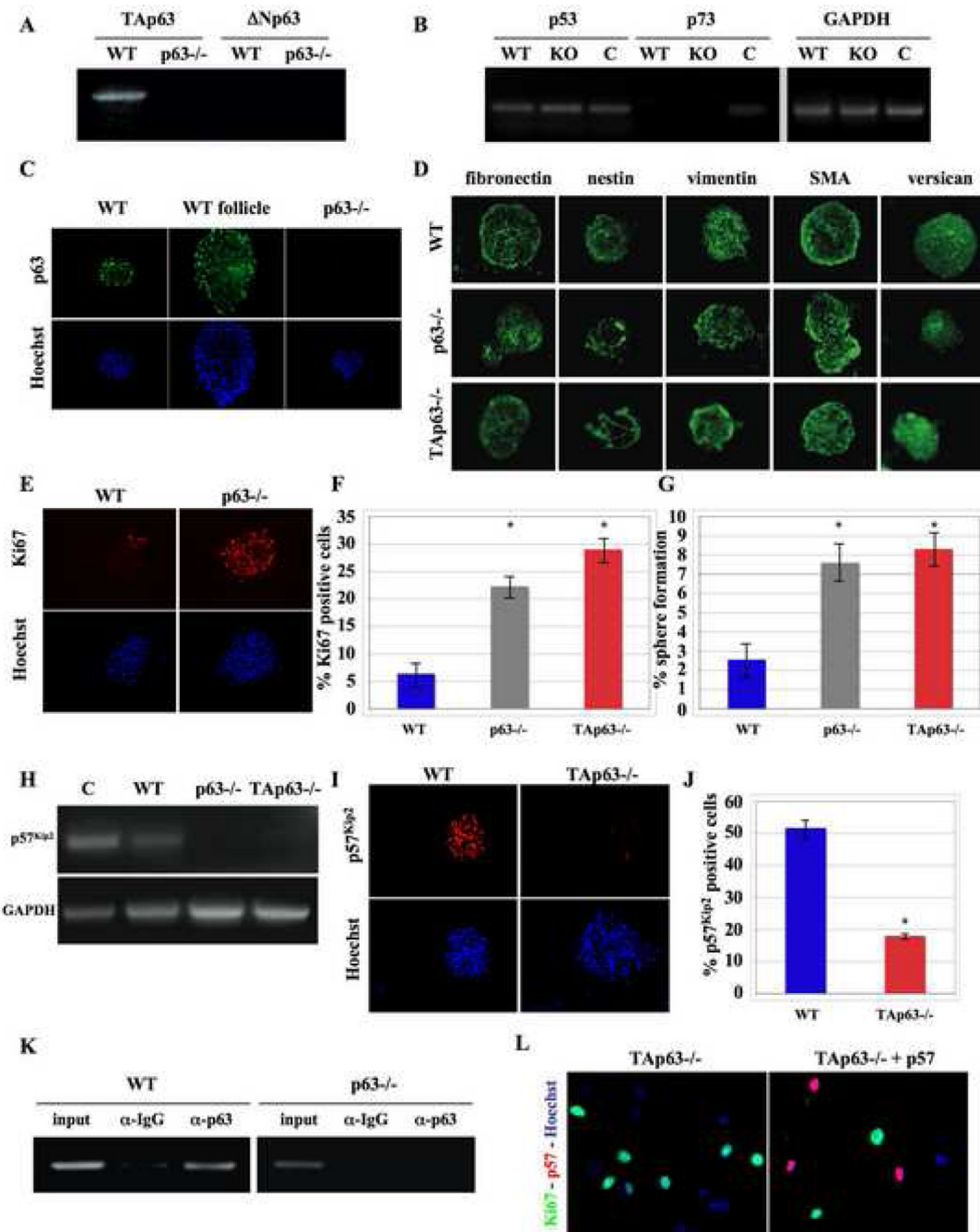


Figure 5. TAp63 regulates self-renewal of dermal precursors via p57^{Kip2}

(A, B) RT-PCR in WT and *p63*^{-/-} SKPs for (A) *TAp63* and $\Delta Np63$ mRNAs and (B) *p53*, *p73*, and *GAPDH* mRNAs. Embryonic day 18 cortical tissue (C) was used as a positive control. (C) Immunocytochemistry for p63 (green) in SKP spheres isolated from WT skin, from reconstituted hair follicles (WT follicle), or from E18 *p63*^{-/-} skin. Hoechst (blue) used as a counterstain. Magnification 400X. (D) SKP spheres isolated from young WT or *TAp63*^{-/-} skin, or from E18 *p63*^{-/-} skin and immunostained for fibronectin, nestin, vimentin, smooth muscle actin (SMA) and versican. Magnification 400X. (E) SKP spheres isolated from neonatal WT skin or from E18 *p63*^{-/-} skin, immunostained for Ki67 (red), and counterstained with Hoechst (blue). Magnification 400X. (F) Quantification of Ki67

positive cells. $n = 3$, $*p < 0.05$. (G) Quantification of cells that form a new sphere at clonal density (2500 cells/ml) in methylcellulose cultures. $n = 3$, $*p < 0.05$. (H) RT-PCR analysis for *p57^{Kip2}* and *GAPDH* mRNAs in E18 cortex (C), young WT and *TAp63*^{-/-} SKPs and E18 *p63*^{-/-} SKPs. (I) SKP spheres isolated from young WT and *TAp63*^{-/-} skin, immunostained for p57^{Kip2} (red) and counterstained for Hoechst (blue). Magnification 400X. (J) Quantification of p57^{Kip2} positive cells. $n = 3$, $*p < 0.05$. (K) ChIP for p63 in young WT or E18 *p63*^{-/-} SKPs and PCR for the *p57^{Kip2}* core promoter. (L) Immunostaining for p57^{Kip2} (red) and Ki67 (green) in *TAp63*^{-/-} SKPs transfected with or without a *p57^{Kip2}* expression vector. Hoechst (blue) was used as a counterstain. Transfected p57^{Kip2}-positive cells were negative for Ki67. Magnification 200X, $n=3$.

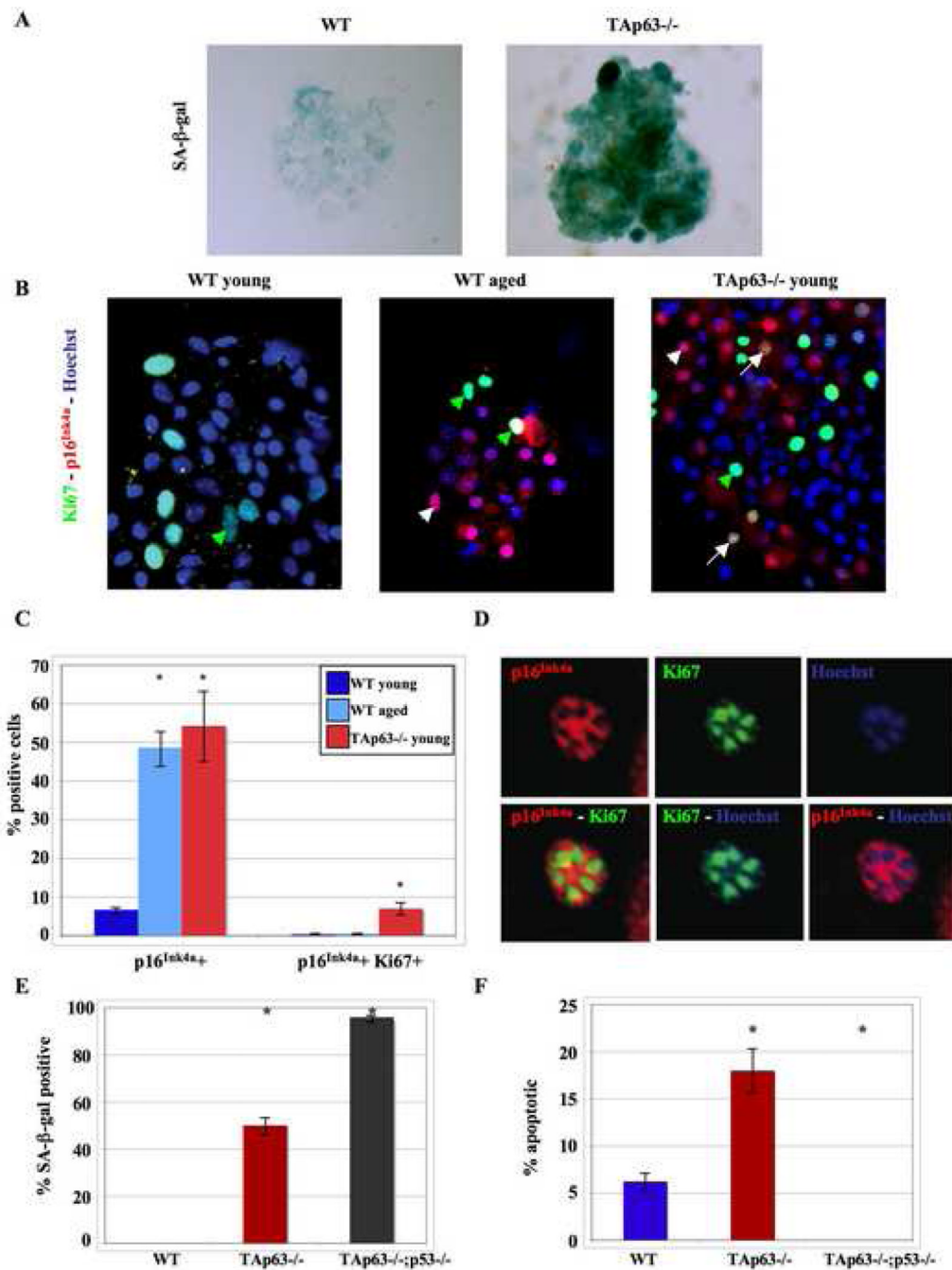


Figure 6. Loss of TAp63 causes dermal precursor cells to senesce

(A) SKP spheres from young WT and *TAp63*^{-/-} SKPs stained for SA-β-gal (blue). Magnification 400X. (B) SKP spheres from young and aged WT and young *TAp63*^{-/-} skin immunostained for p16^{Ink4a} (red) and Ki67 (green) and counterstained with Hoechst (blue). Green arrowheads indicate Ki67, white arrowheads indicate p16^{Ink4a}, and white arrows indicate Ki67 and p16^{Ink4a} double positive cells. Magnification 400X. (C) Quantification of p16^{Ink4a}-positive and p16^{Ink4a}, Ki67 double-positive cells. n = 3, *p < 0.05. (D) High magnification of a *TAp63*^{-/-} SKP cell nucleus that was labeled for p16^{Ink4a} (red) and Ki67 (green) and counterstained with Hoechst (blue). (E,F) Quantification of SA-β-gal positive

(E) or apoptotic (F) keratinocytes in wild-type (WT), *TAp63*^{-/-}, and *TAp63*^{-/-};*p53*^{-/-} cultures. N=3 cell lines for each genotype, performed in triplicate. **p*<0.0001.

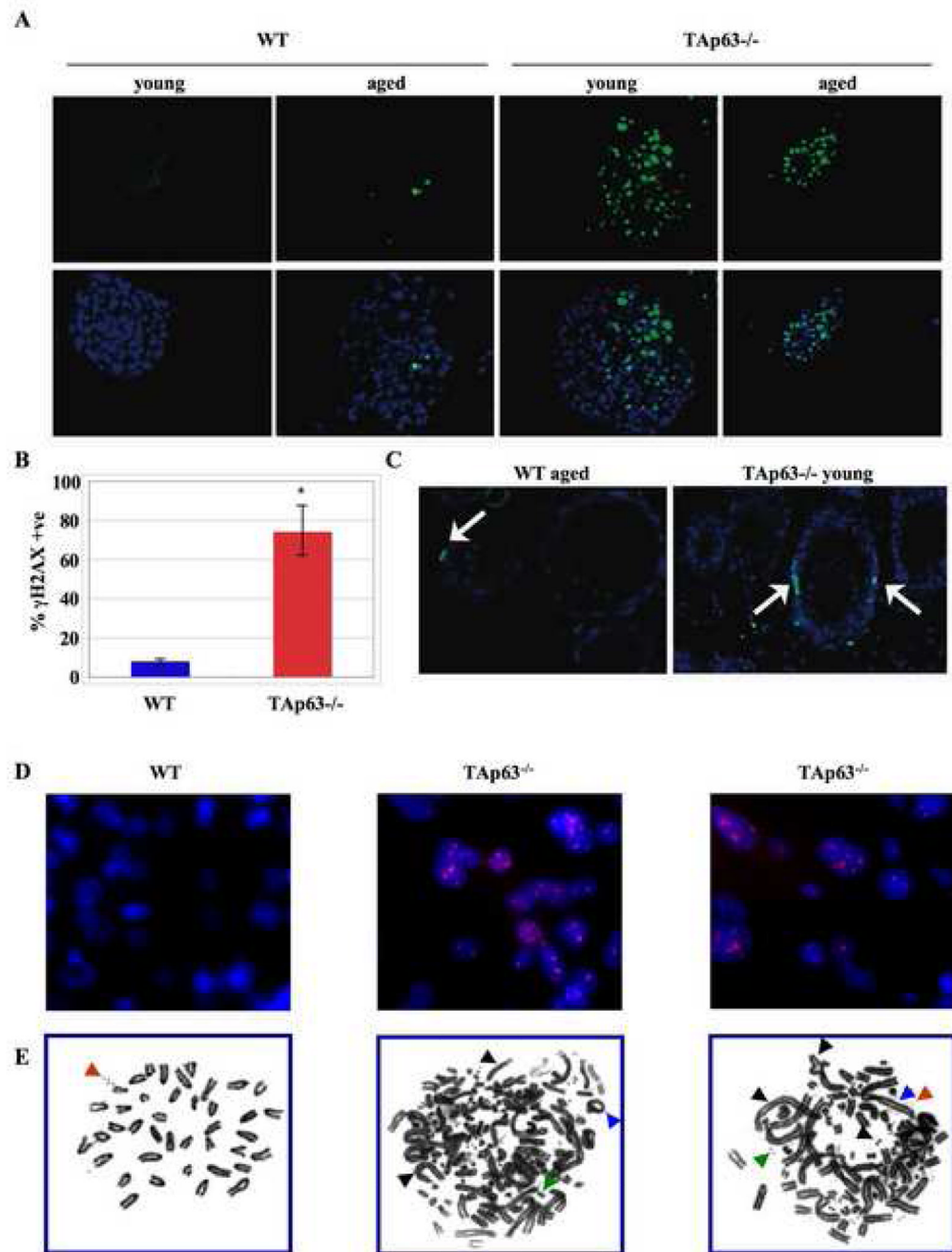


Figure 7. Loss of TAp63 leads to genomic instability

(A) SKP spheres from young and aged WT and *TAp63*^{-/-} skin, immunostained for γ -H2AX (green) and counterstained for Hoechst (blue). Magnification 400X. (B) Quantification of γ -H2AX positive cells. $n = 3$, * $p < 0.05$. (C) Immunostaining for γ -H2AX (green) in aged wild-type and young *TAp63*^{-/-} skin and counterstained Hoechst (blue). Arrows denote hair follicles, and arrowheads indicate positive cells within the dermal sheath. Magnification 200X. (D) Immunostaining for γ -H2AX foci (red) in wild-type and *TAp63*^{-/-} keratinocytes. DAPI was used as a counterstain. (E) Metaphase spreads of wild-type and *TAp63*^{-/-} primary keratinocytes (passage 0). Cytogenetic aberrations in *TAp63*^{-/-} cells are indicated by colored arrows. Chromosomal fusions (black arrows), fragments

(red arrows), breaks (green arrowheads), biarmed chromosomes (blue arrow), ring chromosome (blue arrowhead).